

THE 4TH INTERNATIONAL CONFERENCE ON ALUMINUM ALLOYS

TRACE ELEMENT EFFECTS ON PRECIPITATION PROCESSES AND MECHANICAL PROPERTIES IN Al-Cu-Li-X ALLOYS

D.L. Gilmore and E.A. Starke, Jr.

University of Virginia, Department of Materials Science and Engineering,
Charlottesville, VA 22903-2442, USA

Abstract

The effects of trace additions of indium and magnesium on a modified 2020 Al-Cu-Li alloy have been investigated. Precipitate densities and size distributions were determined by transmission electron microscopy. Tensile yield strengths and Kahn tear toughnesses were obtained for a variety of conditions. Special attention was paid to the effect of precipitation on plastic anisotropy, and comparisons were made with samples which underwent cold work prior to aging. Our studies indicate that with proper heat treatment, indium can play an important role in promoting precipitation hardening in certain applications where a pre-stretch is either not feasible or is deleterious to properties.

Introduction and Background

The mechanical properties of age-hardenable aluminum alloys are controlled primarily by the grain structure and the distribution of appropriate strengthening precipitates within the matrix. The grain structure may be controlled to a large extent by a suitable combination of dispersoid phases and thermomechanical processing [1]. Unfortunately, attempts to control the precipitate structure via variations of the heat treatment are often not successful. In many cases, the material is deformed prior to aging in order to introduce dislocation structures into the matrix which will subsequently act as preferential nucleation sites. However, many product forms do not lend themselves readily to the use of a pre-age stretch and undesirable plastic anisotropy may result. Alternatively, certain trace alloying additions may be used to aid nucleation of the strengthening phases.

Many studies have been made on trace-element effects in Al-alloy systems [2]. Hardy first noted that the tensile properties of Al-Cu-Li alloys were greatly improved by the addition of trace amounts of Cd or In, and to a lesser extent by Sn. He also found that not all phases were affected in the same manner [3, 4]. Silcock subsequently pointed out that cadmium did not seem to affect the properties of alloys with a high Li content [5]. Thus, improvements in yield stress by additions of Cd were seen in modified 2020 alloys (1.2-1.3 wt% Li), but not in 2090 (2.3 wt% Li) [6,7]. Langar and Pickens have more recently found that minor additions of Mg and Ag lead to a uniform, dense precipitation of T₁ particles in an Al-6.3 Cu-1.3 Li alloy [8].

Trace alloying components are thought to alter the nucleation process in four possible ways. They can shift the metastable solvus boundary; they can reduce the volume strain energy

associated with an embryo by straining the matrix interface; if the additions form a new particle, they can reduce the preprecipitate surface energy by providing a heterogeneous nucleation site. Finally, by interaction with vacancies the solute can affect diffusion and formation of clusters which serve as nucleation sites.

It is clear that trace element additions can have a significant effect on precipitation in age-hardenable aluminum alloys. Despite past research, the exact mechanisms responsible for the catalytic role of many trace additions are still poorly understood. The objectives of this investigation are to study the effect of trace additions of indium and magnesium, separately and in conjunction, on the precipitation of the θ' and T_1 phases in an Al-Cu-Li alloy. The presence of Al_3Zr in this system leads to an unrecrystallized grain structure. This in turn produces a sharp texture, which creates undesirable yield anisotropy. The precipitates may have varying effects on this anisotropy due to their different habit planes [9, 10, 11]. We hope to eventually model these phenomena so that predictions might be reliably made for this and other systems.

Experimental Procedure

Materials and Processing

ALCOA provided 3.2-mm-thick rolled sheet of the four alloys. Their chemical compositions are listed in Table I. Samples were found to display optimal properties for a solution heat treatment of one hour at 530 °C. This was followed by quench in cold water. Samples quenched in iced brine did not have notably different properties, indicating a low quench sensitivity. Aging temperatures ranged from 120 °C. to 190 °C., with peak strength occurring for the 160 °C. series. In order to study vacancy effects, some samples were step aged and quenched into a wax bath at 160 °C. Other specimens were subjected to a plastic tensile strain of 3% prior to aging.

Table I. Chemical Composition (Wt. %) of Alloys Studied

Alloy Designation	Cu	Li	Mg	Zr	In	Fe	Si	Al
Al-Cu-Li	4.01	1.24		0.16		0.05	0.04	Bal.
Al-Cu-Li-In	4.06	1.21		0.16	0.09	0.05	0.04	Bal.
Al-Cu-Li-Mg	4.22	1.31	0.54	0.16		0.05	0.04	Bal.
Al-Cu-Li-Mg-In	4.30	1.32	0.55	0.15	0.086	0.05	0.04	Bal.

Microstructure

Precipitate and subgrain structures were investigated using conventional (PHILIPS EM400 operating at 120 kV) and high-resolution (JEOL JEM4000EX operating at 400 kV) transmission electron microscopy. TEM samples were made by mechanical thinning followed by electropolishing in a 3:1 methanol/nitric acid solution cooled to -25 °C., with an applied potential of 15 V. Stereological analysis was done to determine volume fraction and number density of the strengthening phases as well as mean subgrain size.

X-ray diffraction data was taken from $\alpha = 0$ to 80 degrees using center sections of as-quenched samples at (111), (200), and (220) poles in order to quantitatively determine what textures existed prior to aging. Analysis of the x-ray data was performed using the popLA software package [12]. The program was used to convert the data from the three pole figures into an orientation distribution function for each sample [13]. From these functions, theoretical Taylor

factors were calculated for tensile deformation at various angles to the rolling direction, assuming restricted glide.

Mechanical Testing

Initial optimization of the heat treatment was done via Rockwell hardness testing of one-inch squares of the alloy sheet material. Once rough aging curves were obtained in this manner, tensile tests were performed using standard subsize specimens as dictated by ASTM E8. Sample gage lengths were 25.4 mm with a width of 6.35 mm. Tests were performed on specimens cut at 0, 45, and 90 degrees to the rolling direction. In addition, a rough measure of the fracture toughness of the materials was made using Kahn tear tests. Scanning electron microscopy was employed to determine the mode of fracture for each specimen.

Results

Microstructure

Table II indicates the volume fraction, number density, plate diameter and thickness for the θ' (or θ'') particles in the various alloys. Exact numbers for the distribution of T_1 plates are as yet undetermined, but qualitative trends have been observed. In the magnesium-free alloys, indium significantly increases the volume fraction of θ' , although the number density is curiously seen to decrease. The Al-Cu-Li-In samples also contain small amounts of T_1 precipitates. Both magnesium-bearing alloys contain relatively large amounts of the T_1 phase and a high number density of fine θ' particles. T_1 was not observed in the baseline alloy. No S' or δ' precipitates were observed in any specimens. Note that this data was taken at an early stage of aging, well before peak strength is achieved. The bright-field micrographs in Figures 1 and 2 show the respective morphologies of the two precipitates in the different alloys. Small (≈ 5 nm diameter) spherical particles have been noted in the indium-bearing alloys. No firm conclusions as to their composition have yet been reached, although researchers have found In-rich particles serving as nucleation sites in a similar Al system [2, 14]. Subgrain size was seen to decrease substantially in the Mg-bearing alloys, from approximately 2.0 microns to 0.7 microns. Indium shows no such effect on the subgrain structure. Of the four alloys, only the Al-Cu-Li-In samples showed a significant effect on hardness from changing the standard water quench to a wax bath step quench. This decreased the hardness of the test specimens from 32.5 to 28.0 as measured on the Rockwell D scale. It seems that indium does have a relatively strong interaction with vacancies in the Mg-free alloy, but this is in some way negated by the presence of magnesium.

Table II. Precipitate Statistical Analysis - 5 hrs. at 160 °C.

Alloy Designation	Vv (θ')	Nv (θ') ($10^{22}/m^3$)	D (θ') (nm)	t (θ') (nm)
Al-Cu-Li	0.056	9.0	32.2	0.8
Al-Cu-Li-In	0.101	1.7	50.8	3.1
Al-Cu-Li-Mg	0.106	41	19.7	0.9
Al-Cu-Li-Mg-In	0.133	74	18.1	0.7

A representative pole figure from x-ray data is shown in Figure 3. Theoretical Taylor factors, calculated from the x-ray texture data are displayed in Figure 4 as a function of angle to the rolling direction.

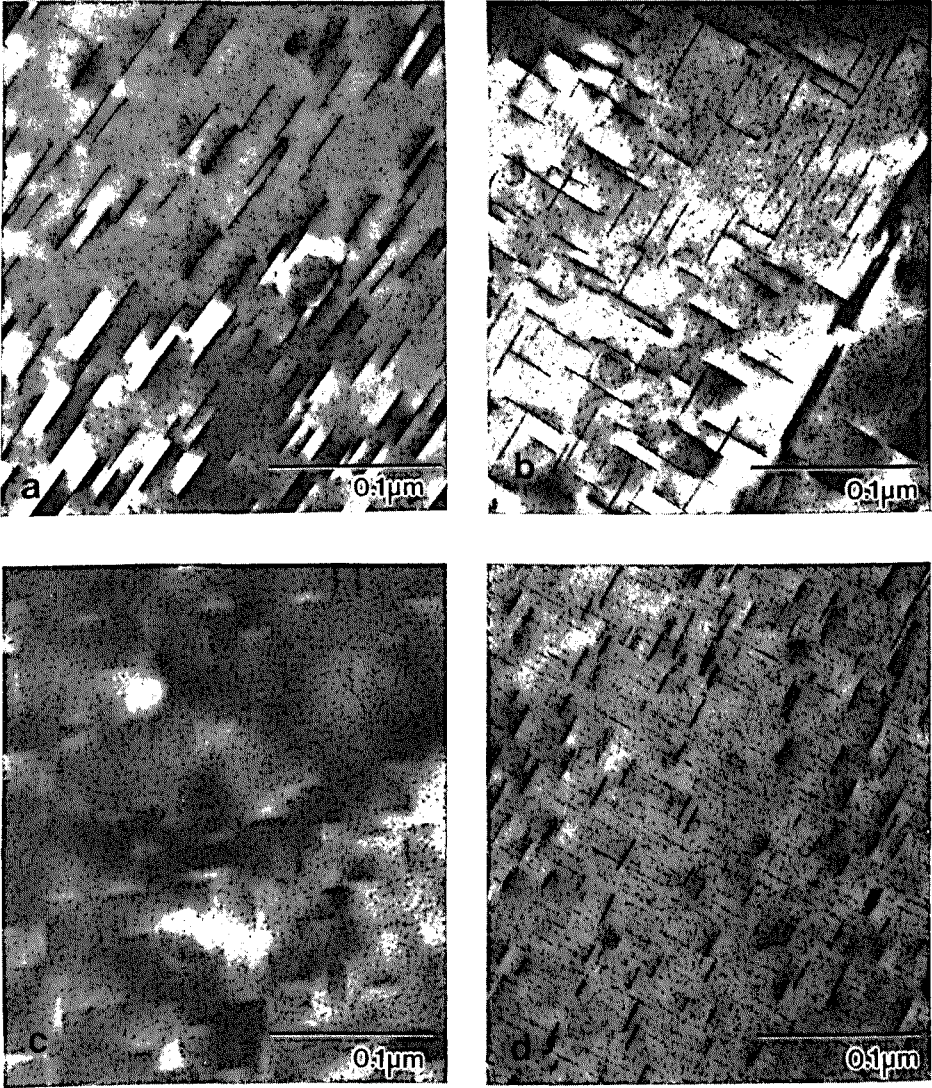


Figure 1. Morphology and distribution of θ' precipitates in: a) Al-Cu-Li; b) Al-Cu-Li-In; c) Al-Cu-Li-Mg; d) Al-Cu-Li-Mg-In. All samples aged for 5 hours at 160 °C. Bright field images with beam direction near [100] axis.

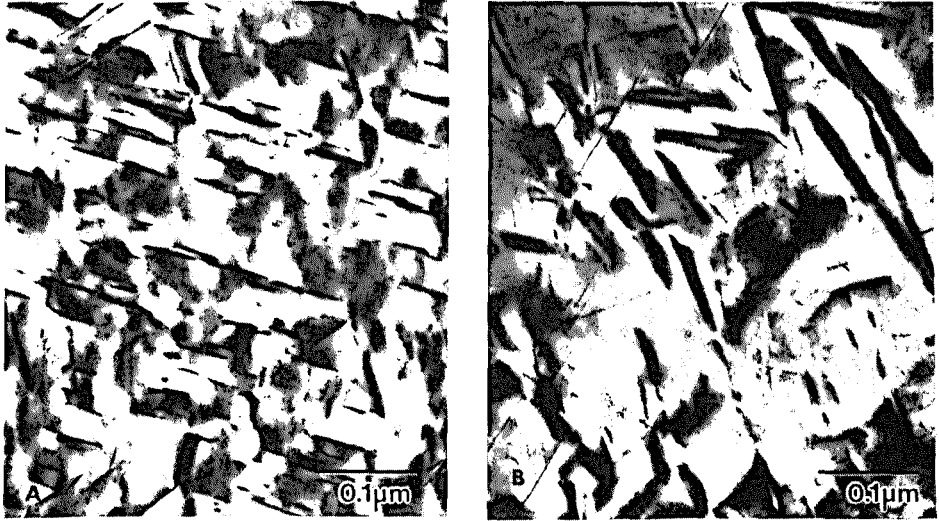


Figure 2. Morphology and distribution of T_1 precipitates in: a) Al-Cu-Li-In, aged 10 hours at 160 °C., dark field image, (220) matrix spot, beam direction near [111]; b) Al-Cu-Li-Mg, aged 24 hours at 160 °C., bright field image, beam direction near [110].

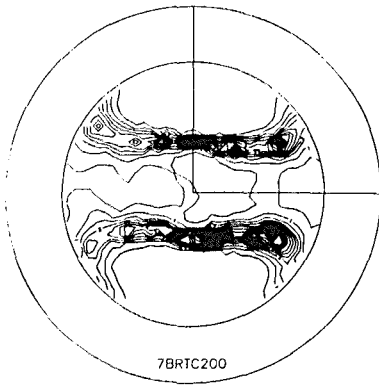


Figure 3. (200) X-ray pole figure taken from center section of as-quenched Al-Cu-Li sample.

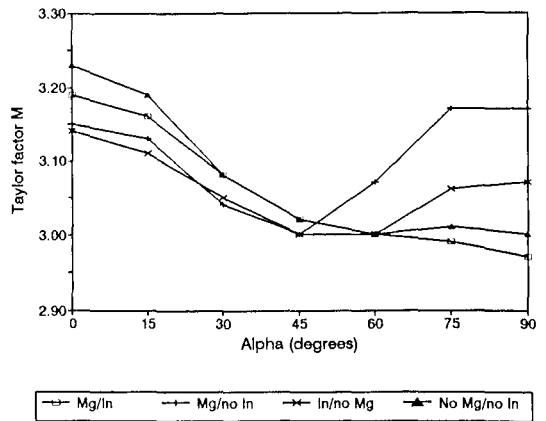


Figure 4. Taylor factors (calculated from x-ray data) plotted versus angle to rolling direction.

Mechanical Properties

The yield strengths for the four alloys in the 3 different orientations are given in Table III. Values are given for as-quenched, peak-age, and peak-age with a 3.0% engineering plastic strain pre-stretch. Time to peak age at 160 °C. was found to be about 32 hours for the Al-Cu-Li-In alloy, 81 hours for the Mg-bearing alloys, and 120 hours for the Al-Cu-Li base alloy. Accelerated aging with the addition of In is not seen in the Mg-free alloy aged at 120 °C., as shown by the aging curves in Figure 5, nor is it seen in the Mg-bearing alloy at any aging temperature. These data points represent an average of 2 to 4 samples each, with care taken to prevent error from natural aging. The ratios of the diagonal and transverse yield stresses to the longitudinal yield stress are shown in Table IV along with the ratios calculated from the as-quenched texture data.

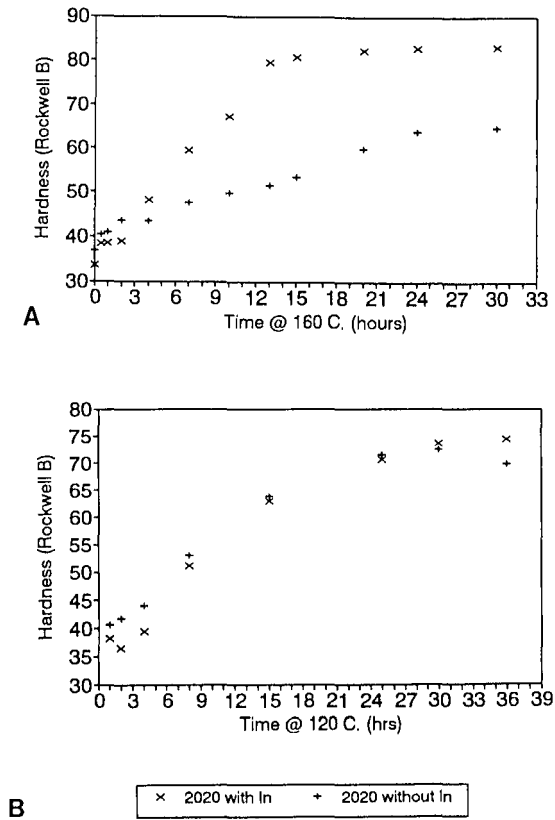


Figure 5. Rockwell hardness vs. time curves for Al-Cu-Li ± In; a) at 160 °C.; b) at 120 °C.

Plotting the ratio of the Kahn tear strength to the yield strength as a function of yield strength shows Al-Cu-Li and Al-Cu-Li-In alloys falling along the same straight line. This indicates that toughness is not adversely affected by the addition of In. This conclusion is supported by SEM fractography work, which shows all samples failing via transgranular shear at peak strength, with some small regions of intersubgranular fracture seen for overaged specimens.

Table III. Yield Strength Data (MPa)

Alloy Designation	As-quenched	Peak Aged	Pre-strain + Peak Aged
Al-Cu-Li			
Longitudinal	160	407	466
Diagonal	145	385	439
Transverse	155	397	454
Al-Cu-Li-In			
Longitudinal	148	505	488
Diagonal	142	469	478
Transverse	155	488	487
Al-Cu-Li-Mg			
Longitudinal	158	532	575
Diagonal	150	487	540
Transverse	164	514	577
Al-Cu-Li-Mg-In			
Longitudinal	157	496	564
Diagonal	151	458	527
Transverse	160	485	564

Table IV. Experimental and Theoretical Anisotropy Ratios

Alloy Designation	As-quenched	Peak-Aged	Pre-strain + Peak Aged	Taylor Prediction
Al-Cu-Li				
Diag., Transv.	.906, .969	.946, .975	.946, .974	.935, .929
Al-Cu-Li-In				
Diag., Transv.	.959, 1.047	.929, .966	.980, .998	.955, .978
Al-Cu-Li-Mg				
Diag., Transv.	.949, 1.038	.915, .966	.939, 1.003	.952, 1.010
Al-Cu-Li-Mg-In				
Diag., Transv.	.962, 1.019	.923, .978	.934, 1.000	.947, .931

Discussion

Indium and magnesium have multiple effects in this alloy system. The data indicate that both promote precipitation of θ' and T_1 . However, the relative size of these effects are different, as might be expected since Mg is present in roughly 30 times greater atomic percentage than In. In the magnesium-free alloy, the promotion of T_1 by indium appears to be secondary to the large increase in the volume percentage of θ' . The θ' precipitates in the Al-Cu-Li-In alloy are larger

than their counterparts in the baseline alloy and seem to have a lower number density, suggesting that they could be limited by the number of heterogeneous nucleating sites available. However, it should be noted that data has at yet only been taken at an early stage of aging, and the precipitate distributions may change with time. As it is unknown whether the θ' precipitates are sheared or looped by dislocations ($t_c \approx 2\text{-}5\text{ nm}$), it is unclear precisely how volume fraction, number density, and particle size come together to give the observed strengthening.

The effect of indium seen in the Mg-free alloy changes in the two Mg-bearing alloys which we have studied. Here T_1 seems to be the dominant precipitate in terms of effect on yield properties. It is unclear what role indium plays with magnesium, but it is now a slightly negative effect, leading us to believe that there may be a significant amount of solute tied up with In and/or Mg which is not available to support the growth of the T_1 particles. Subgrain strengthening may play an additional role. The lack of In effect on precipitation in the magnesium-free alloys at the 120 °C. aging temperature suggests that both Al-Cu-Li and Al-Cu-Li-In are within the metastable solvus boundary at this temperature, whereas at 160 °C. and higher the indium shifts the boundary enough that the indium-bearing alloy lies within while the baseline alloy lies without.

Acknowledgments

The authors wish to thank the Office of Naval Research for providing funding under Grant No. N00014-91-J-1285, Dr. George Yoder, program monitor. One of the authors (DLG) also receives support in the form of a pre-doctoral fellowship from the National Science Foundation.

References

1. J.C. Williams and E.A. Starke, Jr., "The Role of Thermomechanical Processing in Tailoring the Properties of Aluminum and Titanium Alloys" (1982 ASM Materials Science Seminar, Metals Park, OH: ASM, 1983).
2. A.K. Mukhopadhyay, G.J. Shiflet, and E.A. Starke, Jr., Morris E. Fine Symposium, eds. P.K. Liaw, J.R. Weertman, H.L. Marcus, and J.S. Santner (Warrendale, PA: TMS, 1991), 283.
3. H.K. Hardy, J. Inst. Met. **84**, (1955-56), 429.
4. H.K. Hardy, J. Inst. Met. **80**, (1951-52), 483.
5. J. M. Silcock, Phil. Mag. **4**, (1959), 1187.
6. W.X. Feng, F.S. Lin, and E.A. Starke, Jr., Metall. Trans. A **15A**, (1984), 1209.
7. L. Blackburn and E.A. Starke, Jr., Aluminum-Lithium Alloys V, eds. T.H. Sanders, Jr. and E.A. Starke, Jr. (Birmingham, England: MCEP, 1989), 751.
8. T.J. Langar and R. Pickens, Aluminum-Lithium Alloys V, eds. T.H. Sanders and E.A. Starke, Jr. (Birmingham, England: MCEP, 1989), 701.
9. M.A. Przystupa, A.K. Vasudevan, and W.G. Fricke, Jr., Eighth International Conference on Textures of Materials, eds. J.S. Kallend and G. Gottstein (Warrendale, PA: TMS, 1988), 1051.
10. A.K. Vasudevan, W.G. Fricke, Jr., M.A. Przystupa, and S. Panchanadeeswaran, Eighth International Conference on Textures of Materials, eds. J.S. Kallend and G. Gottstein (Warrendale, PA: TMS, 1988), 1071.
11. A.K. Vasudevan, M.A. Przystupa, and W.G. Fricke, Jr., Scripta Metall. **24**, (1990), 1429.
12. J.S. Kallend, U.F. Kocks, A.D. Rollett, and H.R. Wenk, (Los Alamos Natl. Lab., 1993).
13. H.R. Wenk and U.F. Kocks, Metall. Trans. A **18A**, (1987), 1083.
14. R. Sankaran and C. Laird, Mater. Sci. Eng. **14**, (1974), 271.